International Journal of Microwave and Wireless Technologies

cambridge.org/mrf

A broadband circularly polarized antenna for millimeter-wave applications

Yue Xie, Jianping Zhao, Yurong Sun and Juan Xu

Cyberspace Security Academy, Qufu Normal University, Qufu, China

Research Paper

Cite this article: Xie Y, Zhao J, Sun Y, Xu J (2024). A broadband circularly polarized antenna for millimeter-wave applications. *International Journal of Microwave and Wireless Technologies* 1–8. https://doi.org/10.1017/S1759078724000199

Received: 10 July 2023
Revised: 10 January 2024
Accepted: 16 January 2024

Keywords:
antenna array; broadband antenna; circularly polarized (CP) antenna; magnetoelectric dipole (MED); millimeter-wave

Corresponding author: Juan Xu;
Email: xujuan125@163.com

Abstract

This paper presents a broadband circularly polarized (CP) antenna array for millimeter-wave applications, and the antenna array has the advantages of wide impedance bandwidth (IBW), novel CP design, and low profile. The antenna unit consists of a two-layer substrate and two pairs of magnetoelectric dipoles. Stepped microstrip lines coupled by rectangular slits form a feeder network for easy integration. The axial ratio bandwidth (ARBW) is extended because a pair of parasitic patches is loaded and an elliptical perturbation is added. The simulation results show that the antenna has an ARBW of 18.6% (26.4–31.9 GHz) and an IBW of 45.5% (20.6–32.7 GHz), with a gain greater than 7.11 dBic in the IBW. To improve the gain of the antenna, a 2 × 2 antenna array is designed, fabricated, and measured. The measured results show that the array has an ARBW of 16.6% (26.42–31.21 GHz), an IBW of 41.6% (22.28–33.97 GHz), a peak gain of 13.89 dBic in the IBW, the cross-polarization levels in the xoz-plane and yoz-plane are above 20 dB, and a radiation efficiency greater than 89%.

Introduction

With the continuous demand of the market, 4G has gradually failed to meet today's communication needs and 5G came into being. Due to the scarcity of spectrum resources, the design of miniaturized, broadband, high-gain, and array antennas has become a hot topic of research today [1, 2].

Circularly polarized (CP) antenna has the advantages of anti-Faraday rotation effect and anti-multipath interference. It can receive arbitrary line polarization signals and can avoid the mismatch problem caused by polarization mismatch. Therefore, the CP antenna can achieve stable communication transmission, and the CP antenna is needed in many wireless communication systems to transmit and receive signals [3, 4].

In Ref. [5], a low-profile CP magnetoelectric dipole (MED) antenna is introduced, which is excited by a substrate-integrated waveguide aperture coupling feed structure with butterfly-shaped slots. MED antenna consists of a pair of rectangular metal sheets with a square cross-section and elliptical perturbation as electric dipoles and two pairs of vertically metalized vias as magnetic dipoles. The measured antenna array obtains an impedance bandwidth (IBW) of 32.6% and a 3 dB axial ratio bandwidth (ARBW) of 12.5%. The actual measured peak gain is 7.8 dBic. In Ref. [6], a 2 × 2 CP patch antenna array fed by substrate-integrated gap waveguide (SIGW) with sequential rotating phase (SRP) is proposed for broadband millimeter-wave applications. The antenna element consists of a truncated square patch, an SIGW feed line with a three-layer printed circuit board (PCB), and another layer of PCB with air holes for supporting the radiation patch. Each radiating patch is driven by a lower coupling slot engraved on SIGW. By deploying a 2 × 2 SIGW SRP feed network, the wide ARBW is realized, and the measured IBW of the antenna array is 25.6%, 3 dB ARBW is 19%, and high gain of 11.53 dBic. In Ref. [7], a compact broadband CP wearable antenna for wireless body area network in vitro communication is proposed. Loading MED as the parasitic element can improve ARBW and IBW. The measured IBW of the array is 40.8%, 3 dB ARBW is 22.3%, and the actual measured peak gain is 6.5 dBic. In Ref. [8], a broadband CP MED antenna operating in the 28 GHz band is proposed for 5G millimeter wave communication. The geometry of the antenna includes two metal plates, with an extended hook-shaped strip at the main diagonal and two corners of the truncated metal plate at the secondary diagonal. This pair of metal vias connects the improved strip to the ground plane to form a magnetic dipole. L-shaped probe feed between bands is used to excite the antenna. The measured 3 dB ARBW is 18.1%, and the peak gain is 8.5 dBic.

In this paper, a broadband CP antenna unit and an array of millimeter-wave applications in the millimeter band are presented. The antenna unit consists of a two-layer substrate and two pairs of MED [9–11]. Stepped microstrip lines coupled by rectangular slits form a feeder network for easy integration. Loading a pair of parasitic patches and adding elliptical perturbations greatly extends the ARBW. To improve the gain of this antenna in practical applications, a planar 2 × 2 antenna array fed by a four-way microstrip power divider is designed, fabricated, and

© The Author(s), 2024. Published by Cambridge University Press in association with the European Microwave Association

measured. The paper is organized as follows: the second part introduces the structural evolution of the antenna unit, the working principle of CP, and finally gives the simulation results of the antenna unit. The third part gives the physical processing of the 2 × 2 antenna array, all the simulation and measurement results, and the antenna performance comparison table. Finally, a summary is given in the fourth part.

Configuration and operating concepts

Geometry of the antenna

The antenna unit consists of two-layer of Rogers 5880 substrate ($\varepsilon_r = 2.2$, tan $\delta = 0.0009$) and two pairs of MED. Stepped microstrip lines coupled by rectangular slits form a feeder network. The height of the upper dielectric substrate is h_1, and the height of the lower dielectric substrate is h_2. The electric dipole near the rectangular slit is etched with rectangular tangent corners, and the magnetic dipole is three metal vias of radius "R", and the center of the metal vias located in the middle of the three metal vias is offset by a distance of "d_2" from the centers of the other two vias. The other pair of MED is side by side with the first one, with the electric dipoles etching the tangent angles of the triangles and adding elliptical perturbations, the magnetic dipoles are three metal through-holes of radius "R", centered on the same line. The 3D view (Fig. 1a), side view (Fig. 1b), power feed view (Fig. 1c), and radiation patch view (Fig. 1d) of the antenna are shown in Fig. 1.

Operating mechanism

The initial antenna is a pair of MED, a rectangular coupling slot, and a rectangular microstrip line, as shown in Fig. 2a, antenna II is based on antenna I with a rectangular cut angle for the electric dipole, evolution of rectangular microstrip lines into T-shaped microstrip lines, and antenna III is side by side to add a pair of MED and the electric dipole with a triangular cutting angle, evolution of the T-shaped microstrip line into stepped microstrip line. Finally, antenna IV based on antenna III adds an elliptical perturbation, where the axis ratio is obtained by the formula (1), "a" is the long axis of the ellipse and "b" is the short axis of the ellipse:

$$AR = 20 * \lg(a/b) \tag{1}$$

Figure 2b shows that four antennas obtain a wide IBW, and from Fig. 2c, it can be seen that antenna II with a rectangular cut angle to the electric dipole shows the possibility of adjusting to CP, antenna III achieves an ARBW of 8% from 23.16 to 25.12 GHz, while antenna IV with the addition of elliptical perturbation expands the ARBW by 18.6% from 26.4 to 31.9 GHz. The CP principle of antenna realization is equal amplitude in horizontal and vertical directions and a phase difference of 90°. Simulation results of magnitude difference and phase difference of the four antennas are given in Fig. 2d and e. The results show that antenna I does not satisfy the principle of CP, antenna II has the possibility of realizing CP, antenna III has the performance of CP but with narrow ARBW, and antenna IV has equal amplitude and phase difference of −90°. ARBW is wider and the phase difference of antenna IV is −90°, so the designed antenna is a left-hand CP (LHCP) antenna.

Figure 2f simulates the distribution of the surface currents of the four antennas at 29.5 GHz at different times [12]. The antenna I has no obvious rotation of surface current with time at $t = 0$ and $t = T/4$, antenna II has a relatively weak rotation of surface current with time at $t = 0$ and $t = T/4$, antenna III has a clockwise rotation of surface current with time at $t = 0$ and $t = T/4$, and antenna IV has a clockwise rotation of surface current with time at $t = 0$ and $t = T/4$ and strong rotation. The current distributions at $t = T/2$ and $t = 3T/4$ are similar to those at $t = 0$ and $t = T/4$, respectively, but in opposite directions. Combined with the working principle of CP, we can know that the antenna is an LHCP antenna, and after loading a pair of parasitic patches and adding elliptical perturbation, the ARBW is greatly expanded.

The four perturbation structures with the same equivalent area are compared, and the axial ratio results are shown in Fig. 3a;

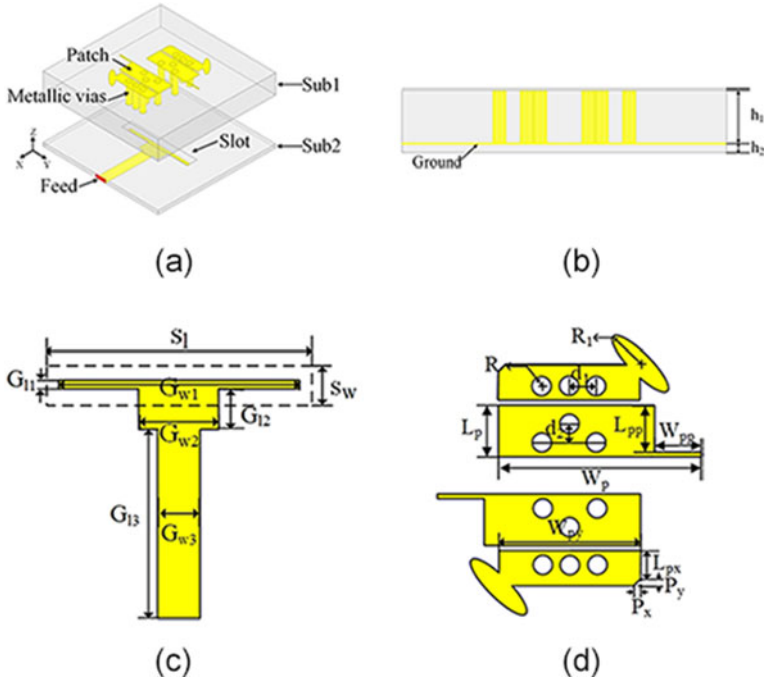

Figure 1. Geometry of proposed CP antenna. (a) 3D view, (b) side view, (c) power feed view, and (d) radiation patch view. $L = 9.5$ mm, $W = 9.5$ mm, $L_p = 1.1$ mm, $W_p = 4.3$ mm, $L_{pp} = 0.97$ mm, $W_{pp} = 1.8$ mm, $R = 0.2$ mm, $R_1 = 0.6$ mm, $d_1 = 0.57$ mm, $d_2 = 0.4$ mm, $L_{px} = 0.75$ mm, $W_{py} = 3$ mm, $P_x = 0.15$ mm, $P_y = 0.15$ mm, $S_l = 5.4$ mm, $S_w = 0.8$ mm, $G_{l1} = 0.2$ mm, $G_{w1} = 5$ mm, $G_{l2} = 0.8$ mm, $G_{w2} = 1.6$ mm, $G_{l3} = 3.8$ mm, $G_{w3} = 0.8$ mm, $h_1 = 0.508$ mm, $h_2 = 0.254$ mm.

https://doi.org/10.1017/S1759078724000199 Published online by Cambridge University Press

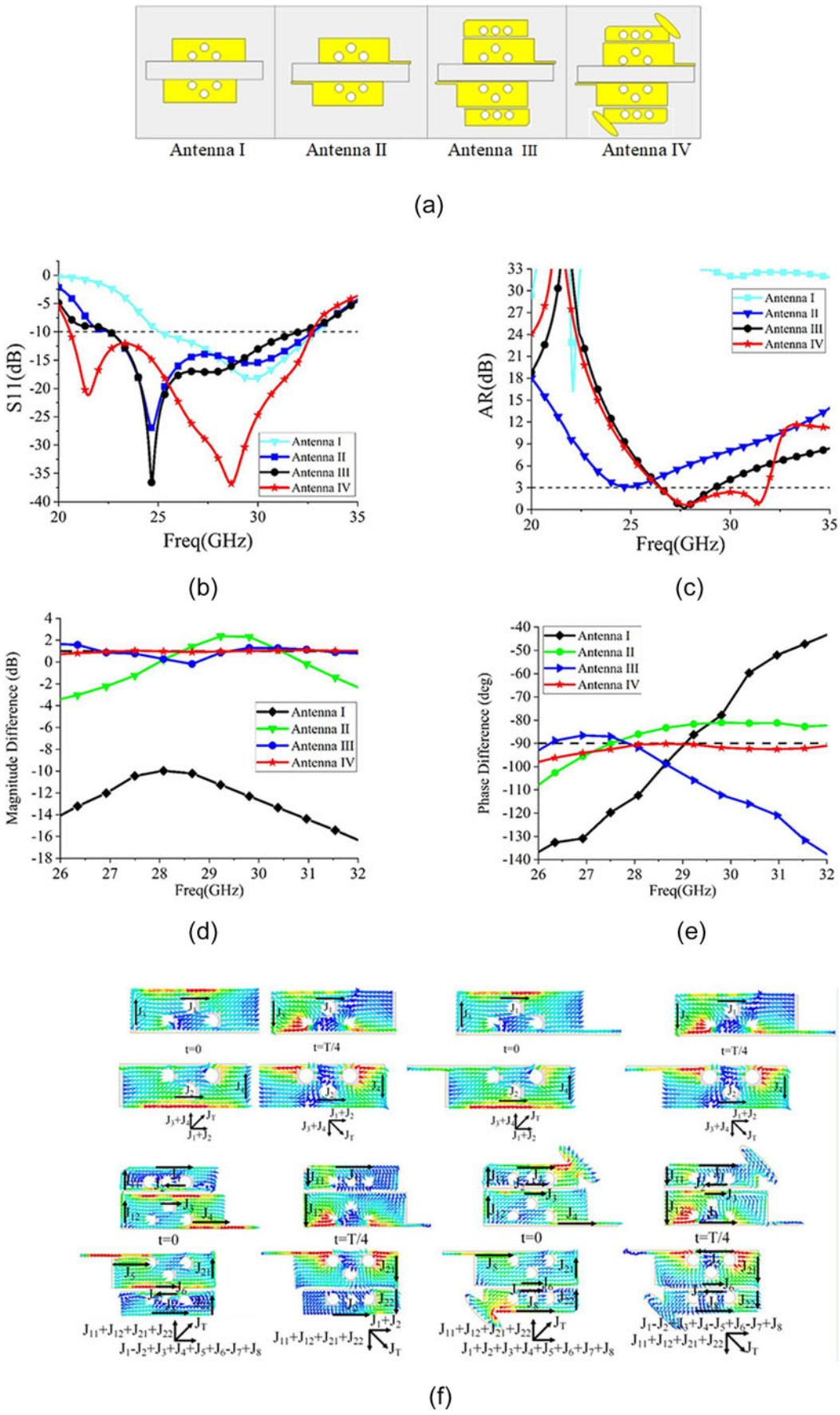

Figure 2. (a) Configuration evolution of CP antennas, (b) a comparison of the reflection coefficient S11 of four antennas, (c) a comparison of the AR of four antennas, (d) a comparison of the magnitude difference of four antennas, (e) a comparison of the phase difference of four antennas, and (f) a comparison of the electric field vector distribution in $T/4$ of four antennas at 29.5 GHz.

https://doi.org/10.1017/S1759078724000199 Published online by Cambridge University Press

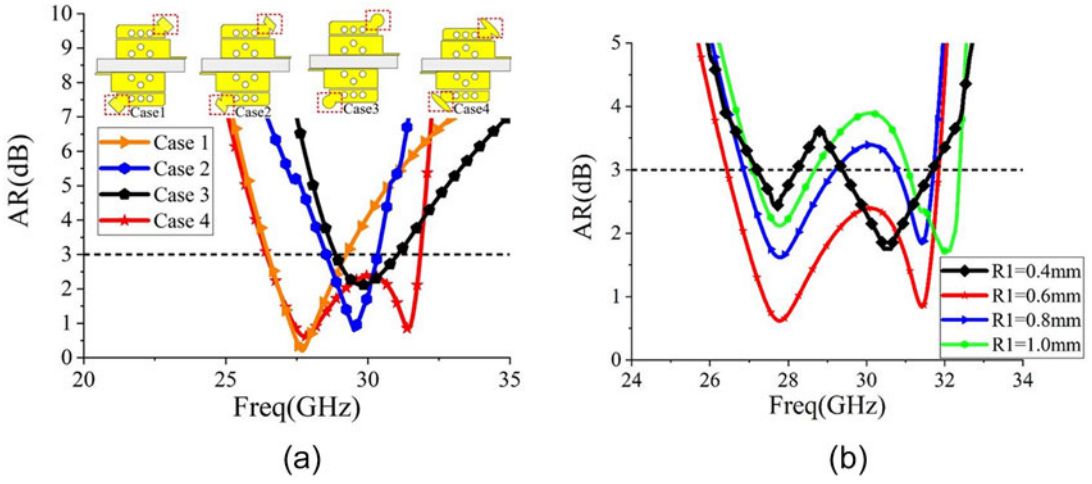

Figure 3. (a) AR of four cases and (b) AR of R_1.

the circular polarization performance when the perturbation structure is elliptical under the same area is best to analyze the parameters of the elliptical long-axis radius, and the axial ratio results are shown in Fig. 3b; and the circular polarization performance is best when the long axis radius $R_1 = 0.6$ mm.

Equivalent circuit model

In order to explain the working principle of the designed CP antenna more clearly, the equivalent circuit characteristics of the CP antenna are analyzed and its model is shown in Fig. 4a. The input port is equivalent to a resistor of 50 Ω, and the feeder line can be equivalent to an inductor L_1 and a series resistor R_1. The input signal passes through substrate 1, which can be equivalent to Tx line 1 and reaches the uppermost radiation patch through the rectangular slot and substrate 2. The rectangular slot is equivalent to the band-pass filter of the inductor (L_2) in series with the capacitor (C_2), and substrate 2 can be equivalent to Tx line 2. The metal via etched in substrate 2 can be equivalent to shunt inductance (L_3), in which the Tx line 2 is connected in parallel. The radiation patch of the antenna can be equivalent to the series connection of radiation resistance (*R*rad), inductance (L_4), and capacitance (C_1). The overall circuit is drawn in Advanced Design System (ADS) software, and the parameters are as follows: $L_1 = 0.6$ pH, $R_1 = 26.8\ \Omega$, $L_2 = 35.5$ pH, $C_2 = 29.7$ fF, $L_3 = 30.5$ pH, *R*rad = 63.8 Ω, $C_1 = 8.4$ fF, and $L_4 = 3.4$ fH. A good agreement between the simulated high-frequency structure simulator (HFSS) response and the numerically calculated advanced design system(ADS) result is observed in Fig. 4b.

The design of the antenna array

To obtain higher antenna gain in the application, a four-way microstrip power divider is designed [13], and four radiating elements are arranged into a periodic structure, which forms a planar 2 × 2 antenna array. The antenna is designed and optimized using Ansys full-wave electromagnetic simulation software. The power divider and the antenna array are shown in Fig. 5a, and the S-parameters of the power divider are shown in Fig. 5b. To investigate the effect of the spacing between the antenna units on the antenna array S11 and AR, a parametric analysis was performed, the results for antenna arrays S11 and AR corresponding to different unit spacing are shown in Fig. 5c. From Fig. 5b, it can be seen that S11 of input port #1 within the IBW of the antenna is lower than −15 dB, #2, #3, #4, and #5 the insertion loss is −6 dB between the four output ports and input port. The isolation between the output ports S23/S45/S25/S34 is lower than −25 dB, which indicates that the mutual coupling between the output ports is weak.

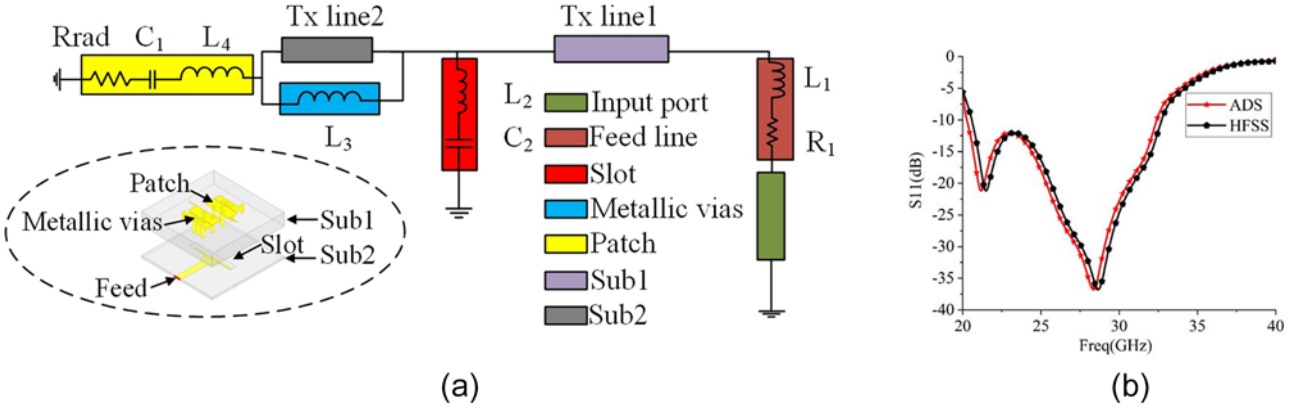

Figure 4. (a) Equivalent circuit modeling and (b) results of ADS and HFSS.

https://doi.org/10.1017/S1759078724000199 Published online by Cambridge University Press

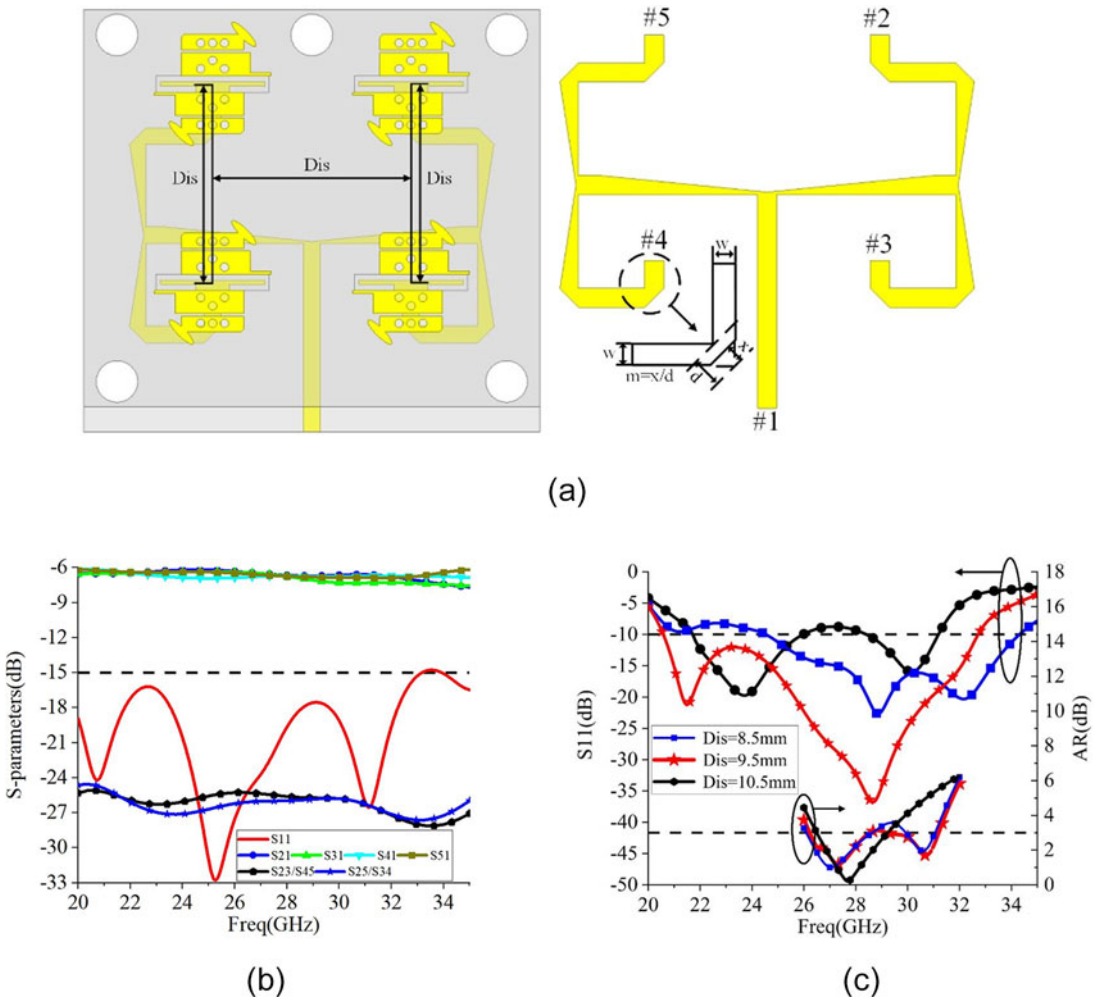

Figure 5. (a) Antenna array and power divider, (b) S-parameters of the power divider, and (c) S11 for different parameters of Dis.

The optimal cell spacing Dis = 9.5 mm can be obtained from Fig. 5c, and five circular holes with DD = 2 mm diameter were etched around the antenna for fixation; to reduce the loss, the compensation structure is designed in the feed network, that is the angle is cut, in which *w, x, d*, and *m* are indicated in Fig. 5a, and the best way to cut the angle can be obtained by formula (2):

$$m = 0.52 + 0.65 \times e^{[-1.35*(w/h)]} \tag{2}$$

where $w = 0.8$ mm, $h = 0.254$ mm, and, therefore, the "m" is calculated at around 0.529.

Next, the gain of the unit or array and the half-power beamwidth are compared, and the result is shown in Fig. 6. The gain increases and half-power beamwidths narrow of antenna arrays. Where the gain can be obtained by the formula (3), "D" is the directivity of the antenna, and "λ_0" is the wavelength:

$$\text{Gain} = 10\lg\left\{4.5*\left(\frac{D}{\lambda 0}\right)\text{^}2\right\} \tag{3}$$

Simulation and measurement

Figures 7a and b show the top view and bottom view of the antenna. Respectively, simulations and measurements were performed for the proposed antenna. Figure 7c shows the simulated and measured S11 as well as the AR of the antenna array. It can be seen that the measured and simulated curves of the antenna match well, and a relative bandwidth of 41.6% (22.28–33.97 GHz) and an ARBW of 16.6% (26.42–31.21 GHz) are obtained. The measured peak gain of the antenna reaches 13.89 dBic as seen in Fig. 7d. The radiation efficiency of the antenna is higher than 89% in the whole operating band. The radiation efficiency can be obtained by the formula (4), where "D" and "Ap" are the directivity and aperture size of the antenna and "λ_0" is the wavelength:

$$\text{Efficiency} = \frac{D\lambda 0\text{^}2}{4\pi Ap} \tag{4}$$

Figures 8a and b give the measured and simulated directional diagrams of the xoz-plane and yoz-plane at 27 GHz and 31.5 GHz. It can be seen that the simulated and measured radiation patterns coincide with each other. The main polarization is LHCP, the right-hand CP (RHCP) level is low, and the measured cross-polarization is below −20 dB in the whole operating band. The antenna achieves a stable radiation performance.

To better illustrate the value of the antenna array designed in this paper for millimeter-wave applications, Table 1 [14–17] shows the comparison of the proposed antenna with other CP antenna arrays in terms of IBW, ARBW, gain, shape, and size. As can be

https://doi.org/10.1017/S1759078724000199 Published online by Cambridge University Press

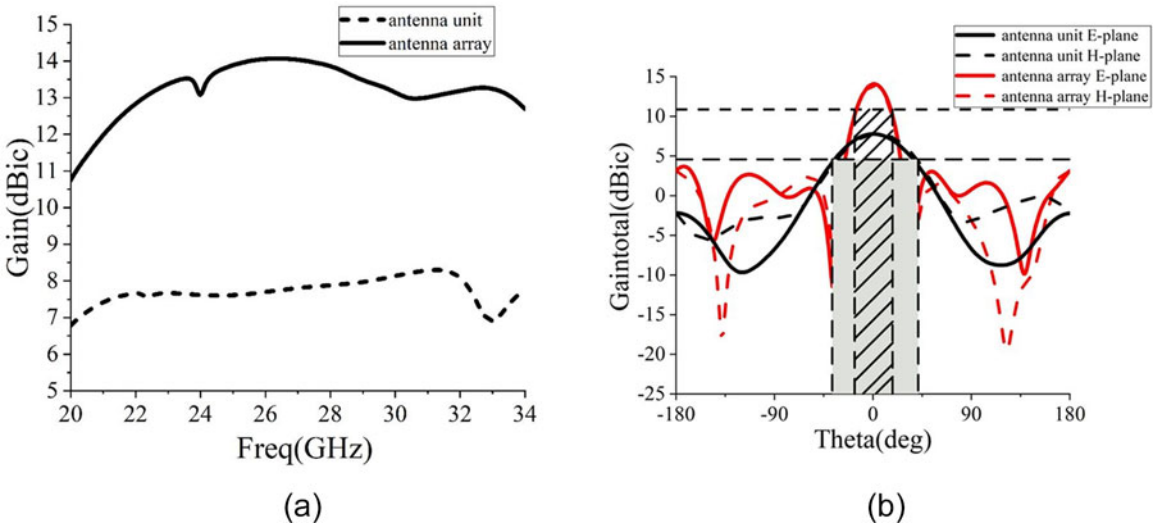

Figure 6. (a) The gain of the antenna unit and array and (b) the HPBW of the antenna unit and array.

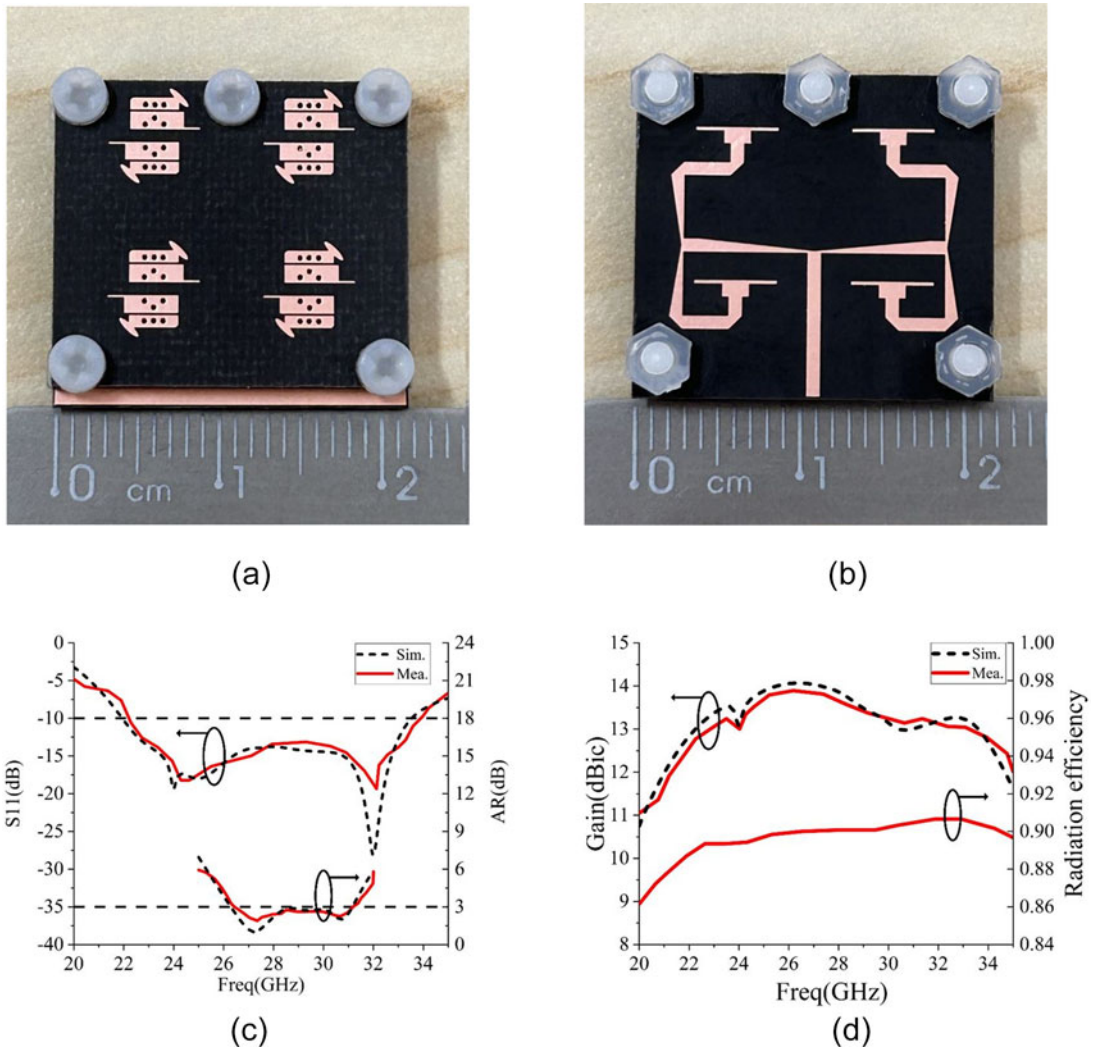

Figure 7. The fabricated antenna and the simulated and measured results. (a) The top view, (b) the bottom view, (c) S11 and AR, and (d) gain and radiation efficiency.

seen from Table 1, the antenna array designed in this paper has significant advantages over arrays of the same size, both in terms of IBW and ARBW, and ensures gain and overall size.

Conclusion

This paper designs and processes a broadband CP antenna unit and array for millimeter-wave applications. The results of the planar

https://doi.org/10.1017/S1759078724000199 Published online by Cambridge University Press

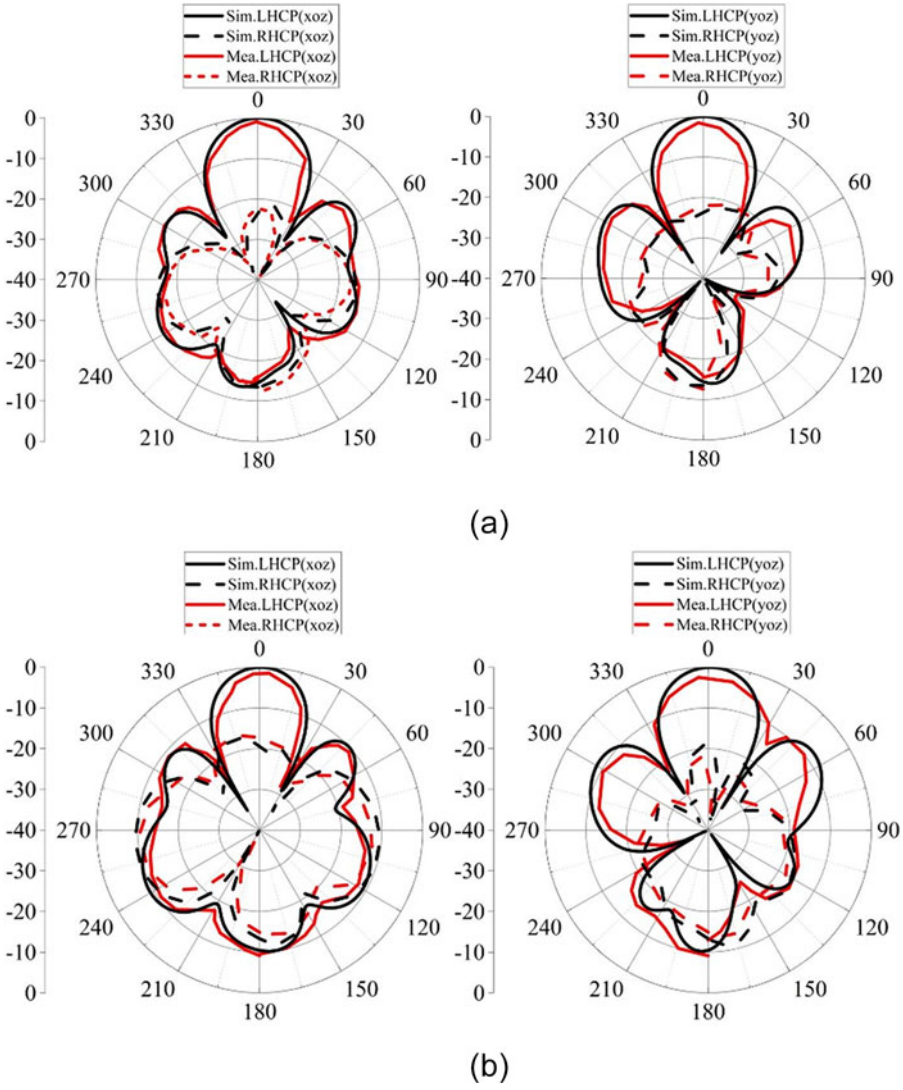

Figure 8. xoz-plane and yoz-plane radiation patterns (a) at 27 GHz and (b) at 31.5 GHz.

Table 1. Performance comparison with the proposed antenna

Ref.	Size (λ_0^3)	Scale	CP center frequency (GHz)	−10 dB bandwidth	3 dB AR bandwidth	Peak gain (dBic)	Cross-polarization ratio
[5]	0.73 × 0.590.12	1	24 GHz	32.6%	12.8%	7.8	≥16 dB
[6]	2.25 × 2.25 × 0.21	2 × 2	25 GHz	25.6%	17.0%	11.53	≥17 dB
[7]	0.64 × 0.64 × 0.17	1	5.8 GHz	40.8%	22.0%	6.50	≥15 dB
[8]	0.83 × 0.83 × 0.23	1	28 GHz	25.4%	18.1%	8.50	≥18 dB
Proposed	2.02 × 1.74 × 0.17	2 × 2	28 GHz	41.6%	16.6%	13.89	≥20 dB

2 × 2 antenna array measurements show that when S11 < −10 dB, the measured IBW is 41.6% from 22.28 to 33.97 GHz. The measured 3 dB ARBW is 16.6% from 26.42 to 31.21 GHz. The peak gain is 13.89 dBic, and the radiation efficiency is greater than 89% in the operating bandwidth. The antenna array is LHCP, with obvious main polarization LHCP and low cross-polarization RHCP level greater than −20 dB, and has good radiation characteristics.

Funding statement. This work was supported in part by the Shandong Natural Science Foundation of ZR2023MF038 and the National Natural Science Foundation of China (61701278).

Competing interests. The author declares that there is no conflict of interest regarding the publication of this paper.

References

1. **Xia J** (2022) China 5G: Opportunities and challenges. *Telecommunications Policy* **46**(2), 102295.
2. **Alsulami MH** (2022) Challenges facing the implementation of 5G. *Journal of Ambient Intelligence and Humanized Computing* **14**, 6213–6226.
3. **Ran J, Jin C, Wang W, Chen J and Wu Y** (2022) Dual-band dual-linearly/circularly polarized shared-aperture antenna for satellite

https://doi.org/10.1017/S1759078724000199 Published online by Cambridge University Press

communication systems. *AEU – International Journal of Electronics and Communications* **148**, 154156.
4. **Zang Z, Zaman AU and Yang J** (2022) Single layer dual circularly polarized antenna array based on ridge gap waveguide for 77 GHz automotive radar. *IEEE Transactions on Antennas and Propagation* **70**(7), 5977–5982.
5. **Wu S, Zhao J and Xu J** (2021) A circularly polarized low-profile ME dipole antenna. *Microwave and Optical Technology Letters* **63**(11), 2852–2858.
6. **Ma C, Ma Z-H and Zhang X** (2019) Millimeter-wave circularly polarized array antenna using substrate-integrated gap waveguide sequentially rotating phase feed. *IEEE Antennas and Wireless Propagation Letters* **18**(6), 1124–1128.
7. **Le TT, Kim Y-D and Yun T-Y** (2022) Bandwidth-enhanced compact circularly-polarized wearable antenna with a magneto-electric dipole. *IEEE Access* **10**, 123225–123232.
8. **Askari H, Hussain N, Sufian MA, Lee SM and Kim N** (2022) A wideband circularly polarized magnetoelectric dipole antenna for 5G millimeter-wave communications. *Sensors* **22**, 2338.
9. **Chen W, Yu Z, Zhai J and Zhou J** (2020) Developing wideband dual-circularly polarized antenna with simple feeds using ME dipoles. *IEEE Antennas and Wireless Propagation Letters* **19**(6), 1037–1041.
10. **Xiang L, Wu F, Yu C, Jiang ZH, Yao Y and Hong W** (2022) A wideband circularly polarized magneto-electric dipole antenna array for millimeter-wave applications. *IEEE Transactions on Antennas and Propagation* **70**(5), 3876–3881.
11. **Ding K, Li Y and Wu Y** (2022) Broadband circularly polarized ME dipole antenna by loading parasitic loop. *IEEE Transactions on Antennas and Propagation* **70**(11), 11085–11090.
12. **Ghosh A, Islam SN and Das S** (2020) A wideband compact antenna with quad-circular polarized bands in its operating regions. *International Journal of RF and Microwave Computer-Aided Engineering* **30**(11).
13. **Bai H, Wang G-M and Zou X-J** (2020) A wideband and multi-mode metasurface antenna with gain enhancement. *AEU – International Journal of Electronics and Communications* **126**, 153402.
14. **Xu R, Li J, Liu J, Zhou SG and Wei K** (2018) UWB circularly polarised slot antenna with modified ground plane and L-shaped radiator. *Electronics Letters* **54**(15), 918–920.
15. **Liu H, Liu Y and Gong S** (2017) Broadband microstrip-CPW fed circularly polarized slot antenna with inverted configuration for L-band applications. *IET Microwaves, Antennas & Propagation* **11**(6), 880–885.
16. **Wei C, Zhou M, Ding K, Yu FX, Mo JJ and Zhao XL** (2018) Compact wideband dual circularly polarized L-shaped slot antenna. *Microwave and Optical Technology Letters* **60**(7), 1685–1691.
17. **Midya M, Ghosh A and Mitra M** (2021) Meander-line-loaded circularly polarized square-slot antenna with inverted-L-shaped feed line for C-band applications. *IET Microwaves, Antennas & Propagation* **15**(11), 1425–1431.

Yue Xie was born in Xingtai, China, in 1997. She received a B.E. degree in Electronic Information Engineering from Qufu Normal University, Qufu China, in 2020. She is currently pursuing an M.E. degree at Qufu Normal University. Her current research interests include 5G millimeter-wave broadband circularly polarized antenna and arrays.

Jianping Zhao is a professor and supervisor of master's students. In 1981, he entered the Physics Department of Qufu Normal University, and in 1988, he pursued a master's degree in Radio and Information Engineering at Wuhan University. His current research interests include wireless communication technology and the design of electronic technology applications.

Yurong Sun was born in Yantai, China, in 1997, and graduated from Qufu Normal University in 2020 with a B.S. degree in Communication Engineering and graduated from Qufu Normal University in 2023 with a M.S. degree in Electronic Information Engineering. Her research interests include millimeter-wave broadband magnetoelectric dipole circularly polarized antennas and arrays.

Juan Xu was born in 1982 and graduated from Nanjing University of Science and Technology in 2016 with a Ph.D. in Electronic Science and Technology. She is currently an associate professor of Cyber Science and Engineering, at Qufu Normal University. Her research interests mainly include microwave/millimeter wave circuits and systems, integrated circuits, antenna array optimization and beam forming, multifunctional electromagnetic metasurface, and terahertz biosensing.

https://doi.org/10.1017/S1759078724000199 Published online by Cambridge University Press